

# The development of a Radiative Transfer Model for waters of varying depth

Ciaran Peyton,<sup>1,\*</sup> Eon O'Mongain,<sup>2</sup> and W.G. Tuohey<sup>3</sup>

<sup>1,2</sup> *School of Physics, College of Engineering, Mathematical, and Physical Sciences, University College Dublin, Belfield, Dublin 4, Ireland.*

<sup>3</sup> *School of Computing, Dublin City University, Dublin, Ireland.*

\*Corresponding author: [peytonc4@gmail.com](mailto:peytonc4@gmail.com)

## Abstract

A new Radiative Transfer Model (RTM) based on Chandrasekhar's solution to the radiative transfer equation in planetary atmospheres has been developed for water applications. The new Radiative Transfer Model offers the possibility of analysing water layers of varying depth with and without bottom reflectance effects. This research is in line with the European Science Foundation's number one recommendation on the remote sensing of coastal environments which is to enhance the quality and quantity of the basic ecosystem parameters retrieved from optical measurements.

A submersible in-situ active portable spectrometry system was developed and used to validate the Radiative Transfer Model in waters of varying depth with a lambertian reflecting bottom.

Comparisons between the model and instrument system measurements for a number of constituent scenarios were undertaken in the laboratory. These include water samples containing varying levels of chlorophyll-*a* and scattering particulates and observation modes involving water layers of varying depth and of varying thickness. This model is shown to provide estimates of basic ecosystem parameters in the laboratory environment with waters of varying depth with a lambertian reflecting bottom.

## 1 Introduction

Chandrasekhar's Radiative Transfer Model (RTM), adapted in this paper to work in water, was developed to describe radiative transfer in atmospheres, particularly plane-parallel atmospheres. In considering transfer problems in plane-parallel atmospheres Chandrasekhar distinguished two cases: (i) the semi-infinite atmosphere which is bounded on one side (at optical depth  $\tau = 0$ ) and extends to infinity in the direction  $\tau \rightarrow \infty$ ; and (ii) the finite atmosphere which is bounded on two sides at  $\tau = 0$  and at  $\tau = \tau_1$ . (Chandrasekhar 1960) For this work the latter case of a finite medium will be analysed.

Chandrasekhar develops a solution to the Standard Problem, one in which a parallel beam is incident on a plane parallel atmosphere at  $\tau = 0$ , and no radiation is incident on the surface at  $\tau = \tau_1$  from below. In the case of an isotropic medium of optical depth  $\tau$ , Chandrasekhar has shown that the emergent radiation just below the  $\tau = 0$  boundary is:

$$L(z = 0, \mu, \tau_1) = \frac{F\mu_0\omega_0}{4(\mu + \mu_0)} (X(\mu, \tau_1)X(\mu_0, \tau_1) - Y(\mu, \tau_1)Y(\mu_0, \tau_1)) \quad \text{Eq1}$$

Where  $L$  = the emergent radiance,  $F$  = Input light flux,  $\mu$  = angle of emergent radiation (Cosine of the zenith angle),  $\mu_0$  = angle of incident radiation,  $\omega_0$  (single scattering albedo) =  $b/(a+b)$ ,  $\tau_1$  (optical depth) =  $(a+b)*z$ ,  $a$  = Absorption coefficient ( $\text{m}^{-1}$ ),  $b$  = total scattering coefficient ( $\text{m}^{-1}$ ) and  $z$  = geometric depth (m).

This is the exact solution where  $X$  and  $Y$  are functions of the geometry, in the sense of the variables  $\mu$  and  $\mu_0$ , and of the optical attenuation of the medium in terms of the variables  $\tau_1$  and  $\omega_0$ . They satisfy a coupled pair of non-linear integral equations

described by Chandrasekhar 1960 in Chapter 8. Numerical values of the  $X$  and  $Y$  functions have been calculated and tabulated for varying values of  $\tau_l$ ,  $\omega_0$ , and  $\mu$  by Sobouti 1963.

As a first approximation one may take  $X(\mu, \tau_l)=1$  and  $Y(\mu, \tau_l) = e^{-\tau_l/\mu}$ . These approximations recover the formulae for the reflected and the transmitted light which has suffered a single scattering process in the atmosphere or medium.

The ‘Standard Problem’ is based on the assumption that there is no radiation incident from below  $\tau_l$ . However the presence of a ground or, in the case of water, a bottom surface at  $\tau = \tau_l$  will modify the top of medium diffuse reflection and also the intensity as measured on the ‘ground’ or ‘bottom’ which will differ from the diffuse transmission in the standard problem. The Planetary Problem describes the situation where at  $\tau_l$  there is a ‘bottom’ which reflects according to Lambert’s law with an albedo  $\lambda_0$ . (Chandrasekhar 1960)

For the isotropic case this gives:

$$L^*(0, \mu, \tau_l) - L(0, \mu, \tau_l) = L_g \gamma_1(\mu, \tau_l) = \frac{\lambda_0}{1 - \lambda_0 \bar{s}} \mu_0 F \gamma_1(\mu_0, \tau_l) \gamma_1(\mu, \tau_l) \quad \text{Eq2}$$

Where  $L^*$  = the emergent radiance with a Lambertian bottom,  $L$  = the emergent radiance without a Lambertian bottom and  $\lambda_0$  = Albedo of the bottom surface.

$$\gamma_1(\mu, \tau_l) = \frac{t(\mu, \tau_l)}{\mu} + e^{-\tau_l/\mu} \quad \text{Eq2a}$$

$$\bar{s} = 2 \int_0^1 s(\mu, \tau_l) d\mu \quad \text{Eq2b}$$

$L_g$  is the constant radiance from the reflecting bottom and is defined by:

$$L_g = \frac{\lambda_0}{1 - \lambda_0 \bar{s}} \mu_0 F \gamma_1(\mu_0, \tau_l) \quad \text{Eq2c}$$

In the foregoing  $s(\mu, \tau_l)$  and  $t(\mu, \tau_l)$  are functions of  $X(\mu, \tau_l)$  and  $Y(\mu, \tau_l)$ :

$$s(\mu, \tau_l) = \mu [1 - \{(1 - x_0)X(\mu, \tau_l) + y_0 Y(\mu, \tau_l)\}] \quad \text{Eq2d}$$

$$\text{and } t(\mu, \tau_l) = \mu [-e^{-\tau_l/\mu} + y_0 X(\mu, \tau_l) + (1 - x_0)Y(\mu, \tau_l)] \quad \text{Eq2e}$$

Where  $x_0 = \frac{1}{2} \omega_0 \alpha_0$ ,  $y_0 = \frac{1}{2} \omega_0 \beta_0$ ,

$$\alpha_i = \int_0^1 X(\mu, \tau_l) \mu^i d\mu \text{ so } \alpha_0 = \int_0^1 X(\mu, \tau_l) d\mu, \text{ and}$$

$$\beta_i = \int_0^1 Y(\mu, \tau_l) \mu^i d\mu \text{ so } \beta_0 = \int_0^1 Y(\mu, \tau_l) d\mu$$

### 1.1 Chandrasekhar’s simplest model for the aquatic medium

As identified above Chandrasekhar has shown that the Isotropic Planetary Problem of a flat surface with known reflecting properties at the bottom of the medium can be reduced to the Standard Problem. The resulting solution or model describes the difference in upwelling emergent radiance with and without a reflecting Lambertian bottom. As described above the exact solution is expressed in terms of  $X$  and  $Y$  functions but as a first approximation one may take  $X(\mu, \tau_l)=1$  and  $Y(\mu, \tau_l) = e^{-\tau_l/\mu}$ . This is the single scattering approximation and is called the ‘simplest model’. This model takes the form:

$$L^* - L = \left[ \frac{\lambda_0}{1 - \lambda_0 \left( \frac{\omega_0}{2} \right) [1 - 2E_2(\tau_1)E_3(\tau_1)]} \mu_0 F \right] * \left[ \frac{\omega_0}{2} E_2(\tau_1) + \left(1 - \frac{\omega_0}{2}\right) e^{-\tau_1/\mu_0} \right] * \left[ \frac{\omega_0}{2} E_2(\tau_1) + \left(1 - \frac{\omega_0}{2}\right) e^{-\tau_1/\mu} \right]$$

**Eq3**

Where  $E_2$  and  $E_3$  are the second and third exponential Integrals respectively, they are calculated using the formula  $E_n(x) = \frac{[e^{-x} - xE_{n-1}(x)]}{n-1}$ .

### 1.2 Separating $L^*$ from $L$ in Chandrasekhar's simplest model

The emergent radiance with a Lambertian bottom,  $L^*$ , is separated from  $L$ , the emergent radiance without a Lambertian bottom, for the single scattering approximation below.

Taking Eq 1 and assuming the simplest model gives:

$$L(0, \mu, \tau_1) = \frac{F\mu_0\omega_0}{4(\mu + \mu_0)} (1 - e^{-\tau_1/\mu} e^{-\tau_1/\mu_0}) \quad \text{Eq4a}$$

Now assuming  $\mu = \mu_0$  and dividing by  $F$ :

$$\frac{L(0, \mu, \tau_1)}{F} = \frac{\omega_0}{8} (1 - e^{-2\tau_1/\mu}) \quad \text{Eq4b}$$

Now taking Eq 3 and assuming again that  $\mu = \mu_0$ .

$$\frac{L^* - L}{F} = \left[ \frac{\lambda_0\mu}{1 - \lambda_0 \left( \frac{\omega_0}{2} \right) [1 - 2E_2(\tau_1)E_3(\tau_1)]} \right] * \left[ \frac{\omega_0}{2} E_2(\tau_1) + \left(1 - \frac{\omega_0}{2}\right) e^{-\tau_1/\mu} \right]^2$$

Finally this gives a model for reflectance  $L^*/F$ .

$$\frac{L^*}{F} = \frac{\omega_0}{8} (1 - e^{-2\tau_1/\mu}) + \left[ \frac{\lambda_0\mu}{1 - \lambda_0 \left( \frac{\omega_0}{2} \right) [1 - 2E_2(\tau_1)E_3(\tau_1)]} \right] * \left[ \left( \frac{\omega_0}{2} \right)^2 (E_2(\tau_1))^2 + \omega_0 E_2(\tau_1) \left(1 - \frac{\omega_0}{2}\right) e^{-\tau_1/\mu} + \left(1 - \frac{\omega_0}{2}\right)^2 e^{-2\tau_1/\mu} \right]$$

**Eq5**

This is the model for the single scattering approximation. With the assumption that  $\mu = \mu_0$ , it corresponds to the reflectance that would be sensed by an active reflectometer illuminating and measuring at the same zenith angle.

### 1.3 Chandrasekhar's solution to multiple scattering

The multiple scattering or exact solution for  $L^*/F$  can be calculated using Chandrasekhar's  $X$  and  $Y$  functions as tabulated by Yousef Sobouti, 1963.

$$\frac{L^*}{F} = \frac{\mu_0\omega_0}{4(\mu + \mu_0)} [X(\mu)X(\mu_0) - Y(\mu)Y(\mu_0)] + \frac{\lambda_0\mu_0}{1 - \lambda_0\bar{s}} \gamma_1(\mu)\gamma_1(\mu_0) \quad \text{Eq6}$$

where:

$$\bar{s} = 1 - [(2 - \omega_0\alpha_0)\alpha_1 + \omega_0\beta_0\beta_1]$$

$$\gamma_1(\mu) = \frac{1}{2} \omega_0\beta_0 X(\mu) + \frac{1}{2} (2 - \omega_0\alpha_0) Y(\mu)$$

Again, if it is assumed that  $\mu = \mu_0$  Eq6 simplifies to:

$$\frac{L^*}{F} = \frac{\omega_0}{8} [\{X(\mu)\}^2 - \{Y(\mu)\}^2] + \frac{\lambda_0\mu}{1 - \lambda_0\bar{s}} \left[ \frac{1}{4} \alpha_0^2 \beta_0^2 \{X(\mu)\}^2 + \frac{1}{2} \alpha_0\beta_0 (2 - \omega_0\alpha_0) X(\mu)Y(\mu) + \frac{1}{4} (2 - \omega_0\alpha_0)^2 \{Y(\mu)\}^2 \right]$$

**Eq7**

This is the model for the multiple scattering approximation and will be compared to the single scattering approximation and to other models of Radiative transfer for waters of a finite depth.

## 2 Comparison of Radiative Transfer models

Inputting different values of  $\omega_0$  and  $\tau_1$  into the single scattering and multiple scattering models results in the reflectance curves as a function of  $\omega_0$  for different values of  $\tau_1$  as shown in Figure 1 below.

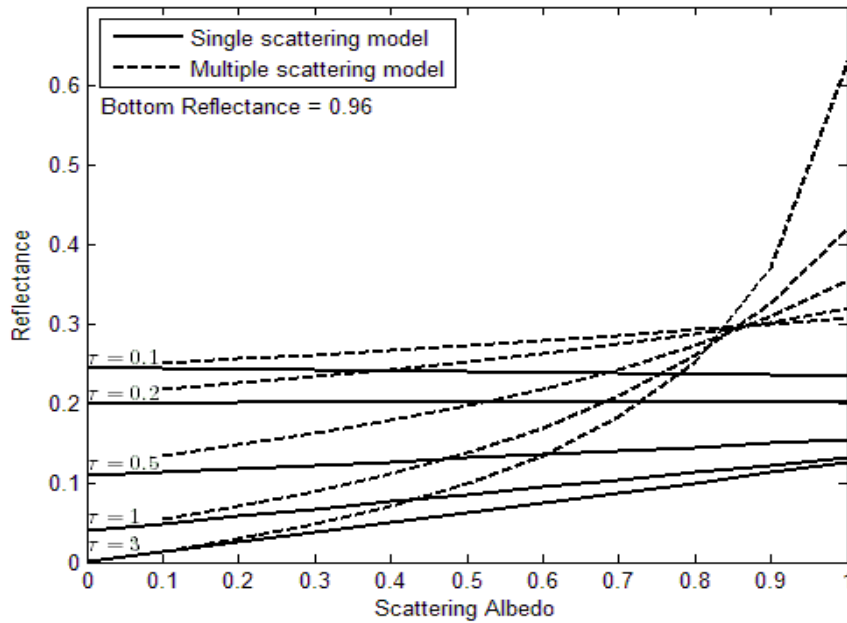


Figure 1. Reflectance versus Scattering Albedo for the single and multiple scattering models for Optical Depth ( $\tau_1$ ) inputs of 0.1, 0.2, 0.5 1 and 3. For a diffusive bottom reflectance of nearly 1 (0.96). The values of the  $X$  and  $Y$  functions for the varying levels of  $\tau_1$  and  $\omega_0$  were calculated using the tables created by Sobouti and interpolated linearly using Delaunay triangulation between table values as required. The values of  $\tau_1$  used are from 0.1 to 3 because this is the range tabulated by Sobouti. It can be seen from the graph that as  $\omega_0$  tends to zero the reflectance output of the single scattering and the multiple models converge for each value of  $\tau_1$ . It can also be seen that the single scattering model predicts a generally linear dependence of reflectance on  $\omega_0$  for all values of  $\tau_1$ . The multiple scattering model only produces linear results for lower values of  $\tau_1$ . For values of  $\tau_1 > 0.2$  the reflectance output of the multiple scattering model begins to increase more rapidly with increasing  $\omega_0$ .

To achieve a better understanding of the variation of reflectance for different water types, some typical water absorption and scattering spectra scenarios were simulated. The pure water absorption spectrum which was compiled from a number of sources by Hakvoort 1994 was used. For a typical constituent the absorption spectrum of Chlorophyll-*a* taken from Bigidare et al., 1990 was used. The chlorophyll spectrum which represents the absorption spectrum of 1  $\mu\text{g/l}$  of chlorophyll is multiplied by 1, 2, 5, 10 and 20 representing a change in chlorophyll level in the water of 1  $\mu\text{g/l}$ , 2  $\mu\text{g/l}$ , 5  $\mu\text{g/l}$ , 10  $\mu\text{g/l}$  and 20  $\mu\text{g/l}$ . This is a simulation of absorption of chlorophyll\_ *a* at 675 nm based on the results of Bidigare, and does not include the absorption and scattering of phytoplankton cells.

The scattering scenario is represented by scattering in NTU which was converted to scattering coefficient  $b$  based on a technique developed by Zaneveld et al 1980 and

used here with results obtained from a spectral reflectometer instrument as described by Peyton 2010. The empirical relationship between NTU and  $b$  is given below:

$$b = 0.1315(NTU) + 0.13766 \quad \text{Eq 8}$$

In the results in Figure 2, the background grey lines are from Figure 1 above; this is to show the variation of the simulated water absorption and scattering values along similar scales.

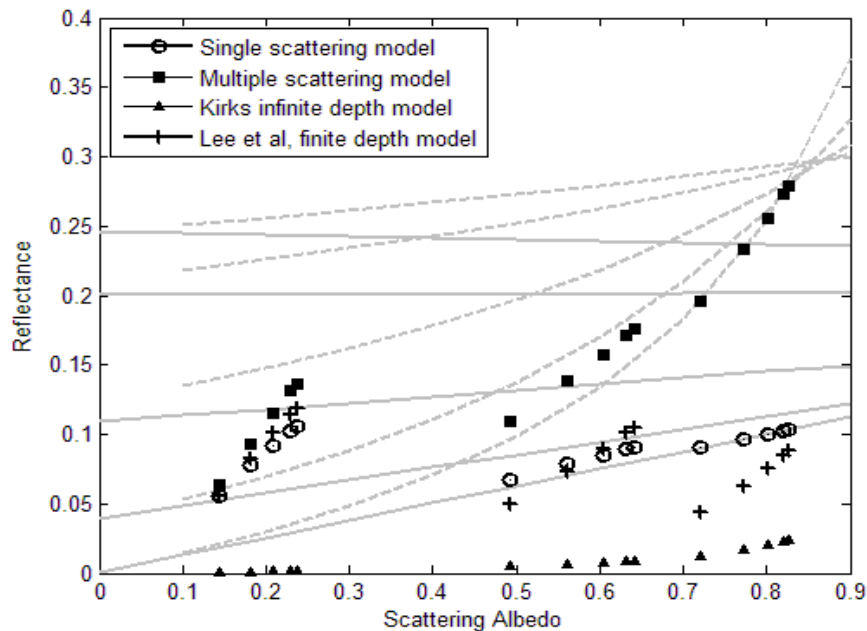


Figure 2. Reflectance versus Scattering Albedo for the single scattering model, multiple scattering model, Kirks infinite model and Lee et al finite depth model. For water of depth 1 meter with a Reflecting Lambertian bottom of reflectance 0.96. For each set of data points the chlorophyll values are  $1\mu\text{g/l}$ ,  $2\mu\text{g/l}$ ,  $5\mu\text{g/l}$ ,  $10\mu\text{g/l}$  and  $20\mu\text{g/l}$ . The four series at scattering albedos near 0.2, 0.55 and 0.75 represent the scattering caused by turbidities of 0, 5 and 15 NTU respectively.

Kirks model (Kirk 1994) and Lee's approximation (Lee et al., 1998; Lee et al., 1999), require knowledge of backscattering rather than scattering coefficient. This comparison assumes that backscattering ' $b_b$ ' is 6% of scattering ' $b$ '. This assumption however is known to be variable with aquatic environment. (Sydor et al., 2002; Snyder et al., 2008)

A chlorophyll level of  $1\mu\text{g/l}$  corresponding to lowest absorption gives the highest reflectance for all data sets and the higher absorption at  $20\mu\text{g/l}$  corresponds to the lowest reflectance.

It can be seen from Figure 2 that Kirks model gives a lower value of reflectance for low scattering levels; again this is expected since Kirks model is for infinite depth and at lower NTU levels the bottom effect is going to add considerably to reflectance. The other three models are all in good agreement for lower levels of NTU. At higher levels of scattering the multiple scattering model predicts a higher reflectance than the others. Also at these higher values of NTU the bottom would be expected to have less effect as Kirks infinite model agrees quite well with Lee's finite approximation.

### 3 Materials and Methods

There is a requirement for a small and inexpensive remote sensing instrument that can provide a profiling capability in the water; that is for an instrument that could measure both, at or above the surface and submerged to provide a profiling capability. Thus a submersible Active Reflectance Spectroscopy system is required. The AquaPod™

instrument was designed and developed to provide in-situ active spectral remote sensing data from the water.

The instrument contains a spectrometer designed specifically for this task using optical design software. The prism spectrometer design has optical fiber input and covers the visual and NIR spectrum. The wavelength range used in the following analysis is from 500nm to 800nm. The instrument is described in Peyton 2010.

### 3.1 Experimental Setup

An experiment was devised to validate the Radiative Transfer Equation using the new AquaPod™ instrument. The measurements are taken using a cylindrical black plastic tank. The black sides and bottom of the tank reduced the possibility of any unwanted reflectance. The tank is filled with water up to a height 0.5m, with a total volume of water of 80 litres. The AquaPod™ Instrument is placed just below the water surface to eliminate any surface reflectance. The light source and optical fibres are located together at the front face of the instrument. The instrument is placed at a 10° zenith angle. The reflectance surface is an Aluminium disk of 0.18m radius. Both sides of the disk have been sanded to give a near Lambertian reflectance. One side is painted matt black and the other painted matt white.

Using Chandrasekhar's Simplest Model from Eq3;  $L^*-L$  is the measured signal from the Lambertian Reflecting Bottom (simulated here using the white tile surface) minus the signal from when no light returns from the bottom (simulated here using the black side of the tile surface). The measurement was carried out for depths of 0.1m, 0.2m, 0.3m 0.4m and 0.5m for both sides of the surface. This was carried out for varying levels of absorption 'a' and scattering 'b'. If scattering is not high 'L' will be very low. These Chlorophyll and Scattering levels were measured using the ChloroFlow instrument described in CEN/TC 230. The quantities of chlorophyll used were 59.43, 40.88, 20.45, 10.93µg/l. The scattering quantities used were 16, 12, 8, 4 NTU. The input light flux ( $F$  term in Eq3) cannot be measured using this instrument and so to match the measurement to the Model this term must be removed. The process for doing this will be called the Log Ratio Method.

$$\left[ \text{Log} \left( \frac{L^*_{z1} - L_{z1}}{L^*_{z2} - L_{z2}} \right) \right] \quad \text{Eq9}$$

In Eq9 above  $z1$  is the higher depth and  $z2$  is the lower depth. Since the input light will be the same for both depths the  $F$  term can be dropped from the Model Equation. Using the Log Ratio Method the measurements can be directly compared to the Model for different depths and measurement layer thicknesses with varying constituent levels.

## 3 Results

Inversion methods were used to get an estimation of absorption using the new AquaPod™ instrument and Chandrasekhar's Simplest Model. The correlation between the chlorophyll measurements taken with the ChloroFlow instrument and estimated absorptions from the AquaPod™ and Model were analysed.

Figure 3 shows that there is a good correlation between the chlorophyll measurement and the estimated absorption for a layer of water from 0.2 to 0.3m.

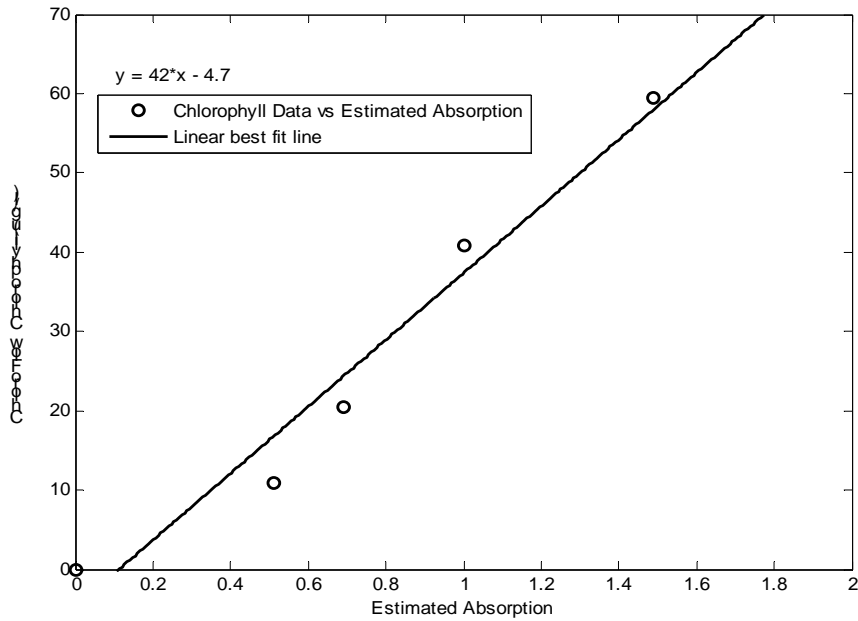


Figure 3. ChloroFlow Chlorophyll measurements against Estimated Absorption at 675nm layer from 0.2m to 0.3m.

Figure 4 shows a graph of the chlorophyll level against the estimated absorption for a water layer of thickness 0.2m.

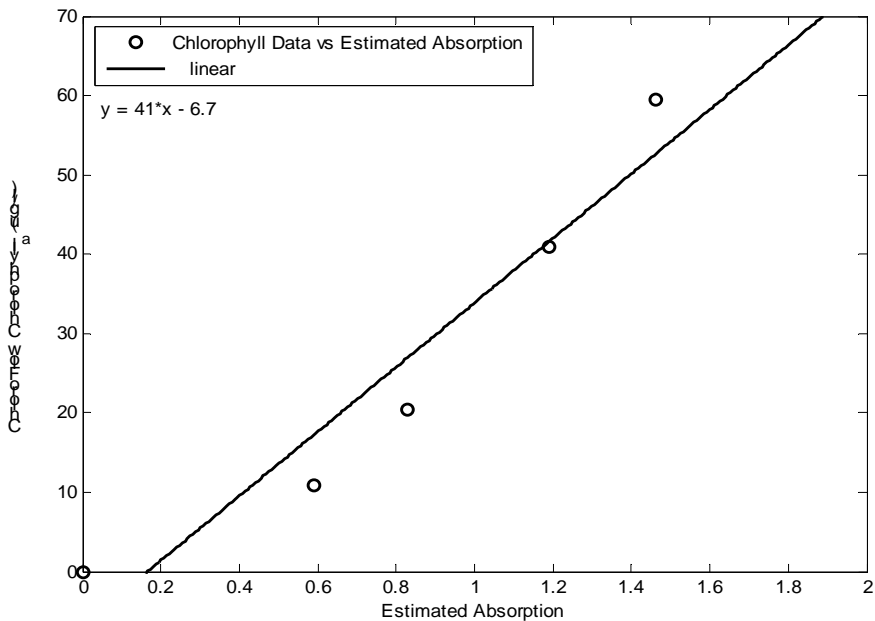


Figure 4. ChloroFlow Chlorophyll measurements against estimated absorption at 675nm layer of thickness 0.2m.

The graph shows that the estimated absorption is consistent no matter what thickness of the water layer is analysed. The origin was added to the data points for the best fit line.

#### 4 Conclusion

A single scattering model and a multiple scattering model have been developed for the aquatic medium based on Chandrasekhar's work on planetary atmospheres. The models were formulated for waters of finite depth incorporating the effects of bottom reflectance for an assumption of isotropic scattering. For this analysis surface

reflectance effects have not been included. These models have been compared with Kirks model of subsurface reflectance for waters of infinite depth and with Lee's model for waters of finite depth with a lambertian reflecting bottom. The models can be used with inversion techniques to produce constituent estimate from remotely sensed data taken in shallow waters.

From the different models described above there is the possibility to study the relationship between scattering and backscattering. Using inversion techniques an estimate of scattering can be obtained using the single and multiple scattering models. Similarly an estimate of backscattering can be obtained for the same water using Kirks or Lee's models described above. Comparing these for different water types may be used to give a more detailed understanding of the relationship between scattering and backscattering coefficients.

Future work is possible through applying Chandrasekhar's findings on single scattering and multiple scattering models for non-isotropic cases. In this regard closed-form approximations such as those of Tuohey 2005 (semi-infinite medium) could, where available, be substituted for tabulated functions. For future work on the isotropic case a more detailed table of X and Y functions for a wider range of input  $\omega_0$  and  $\tau_1$  values would improve the multiple scattering models performance.

## References

- Bidigare, R. R., Ondrusek M. E., Marrow J. H. and Kiefer D. A., "In vivo absorption properties of algal pigments," in *Proc. SPIE* **1302**, (Ocean Optics X 1990)
- Chandrasekhar, S., *Radiative Transfer*, (Dover, 1960).
- Hakvoort J.H.M., *Absorption of light by surface water*, (Thesis, Delft University Press, 1994)
- Kirk J.T.O., *Light and Photosynthesis in Aquatic Ecosystems, Second edition*, (Cambridge University Press 1994)
- Zhongping Lee, Kendall L. Carder, Curtis D. Mobley, Robert G. Steward, and Jennifer S. Patch, "Hyperspectral Remote Sensing for Shallow Waters. I. A Semianalytical Model," *Appl. Opt.* **37**, 6329-6338 (1998)
- Zhongping Lee, Kendall L. Carder, Curtis D. Mobley, Robert G. Steward, and Jennifer S. Patch, "Hyperspectral Remote Sensing for Shallow Waters. 2. Deriving Bottom Depths and Water Properties by Optimization," *Appl. Opt.* **38**, 3831-3843 (1999)
- Peyton C., *Portable Spectrometer System for Characterising the Optical Properties of Water*, (Thesis, University College Dublin, 2010)
- William A. Snyder, Robert A. Arnone, Curtiss O. Davis, Wesley Goode, Richard W. Gould, Sherwin Ladner, Gia Lamela, William J. Rhea, Robert Stavn, Michael Sydor, and Allen Weidemann2 Optical scattering and backscattering by organic and inorganic particulates in U.S. coastal waters *Appl. Opt.* **47**, No. 5 \_ 666-677, (2008)
- Sobouti Y., "Chandrasekhar's X-, Y-, and related functions," *Astrophysical Journal Supplement* **7**, 411-560 (1963).
- Sydor M., Wolz B. D., and Tharlow A. M., Spectral Analysis of Bulk Reflectance from Coastal Waters: Deconvolution of Diffuse Spectra Due to Scattering and Absorption by Coastal Water," *Journal of Coastal Research* **18**, 352- 361 (2002)
- Tuohey W. G., "Picard style iteration for anisotropic H-functions," *Journal of Quantitative Spectroscopy and Radiative Transfer* **96**, 85-101 (2005)
- Zaneveld J.R.V., Spinrad R.W., Bartz R., "Optical properties of turbidity standards," in *Proc. SPIE* **208**, (Ocean Optics VI 1980)
- CEN/TC 230 N 623; Date: 2009-04; NWIP Working Document: prEN In vivo chlorophyll; 2009; CEN/TC 230